Brazilian Journal of Physics

***versão impressa* ISSN 0103-9733**

Braz. J. Phys. v. 27 n. 4 São Paulo Dez. 1997

http://dx.doi.org/10.1590/S0103-97331997000400012

Electron Cyclotron Absorption by RF Driven Current-Carrying Plasmas With Fast Particle Losses

P. R. da S. Rosa
Departamento de Física, UFMS, Caixa Postal 649,
79070-900 Campo Grande, MS, Brazil
e-mail: rosa@dfi.ufms.br

L. F. Ziebell
Instituto de Física, UFRGS, Caixa Postal 15051,
91501-970 Porto Alegre, RS, Brazil
e-mail: ziebell@if.ufrgs.br

Received June 22, 1997

We use quasilinear theory to investigate the influence of losses of energetic particles on the behaviour of electron cyclotron absorption during lower hybrid plus electron cyclotron current drive. Our analysis takes into account the quasilinear effects of the interaction of electron cyclotron radiation with a lower hybrid produced tail in the presence of collisions and a loss term for energetic particles. We study the behaviour of different quantities, as the parallel electron distribution function and the perpendicular temperature, for several values of the electron confinement time, an important parameter of the model loss term. The absorption of extraordinary mode electron cyclotron waves by tail electrons results to be substantially reduced when the loss term is taken into account in the quasilinear diffusion equation, as compared to the case where these losses are neglected.

I. Introduction

The influence of particle losses in the behaviour of current drive by lower hybrid waves, and the general problem of interaction of RF waves with magnetized plasmas in general, have been studied by several authors [1-9]. In particular, experimental results obtained in present days tokamaks have shown that the efficiency of lower hybrid current drive is smaller than the ideal value predicted by Fisch and Boozer theory [10]. This discrepancy has been attributed to the finite confinement time of fast electrons, and it has been predicted that the ideal theoretical efficiency would be recovered for future fusion devices, with improved confinement times [1]. Extrapolation due to experimental results found for the JT-60U tokamak [5] also supported the prediction that for large machines the power loss due to loss of energetic particles will not be important during lower hybrid current drive.

Other features, however, may be influenced by losses of energetic particles, and may eventually affect the efficiency of current generation. From this point of view, it is of particular interest for electron cyclotron current drive and heating to understand the influence of losses of energetic particles, mainly those particles belonging to the superthermal tail of the electron distribution function, on the electron cyclotron absorption coefficient. As pointed out elsewhere [11-13], the absorption coefficient for electron cyclotron waves is the outcome of a delicate balance between competitive effects. In particular, when electron cyclotron and lower hybrid waves are present in the system, the increasing population of particles along the cyclotron resonance curves may compensate the decrease in the value of the electron cyclotron absorption coefficient provoked by the quasilinear flattening of the electron distribution function and consequent decrease of its parallel and perpendicular derivatives. For instance, it has been shown that the asymptotic absorption coefficient for extraordinary mode waves may increase after the introduction of electron cyclotron waves, for sufficiently large angle of injection relative to the normal to the magnetic field [12]. The loss of fast particles due to spatial transport affects the distribution of particles in momentum space, and may therefore be an important factor to be considered in the balance, in order to describe the evolution of the absorption coefficient [14-16].

These considerations point out to the interest of a investigation of the time evolution of the electron distribution function under the effect of electron cyclotron and lower hybrid waves, in the presence of collisions and fast particle losses, in order to study the effects of the competition between several effects, like the quasilinear flattening of the distribution function, the raising in the tail electron population, and the extraction of energetic particles from the tail, on the absorption coefficient of electron cyclotron waves. In the present paper we describe the results of our investigation of the subject, obtained by numerical solution of the Fokker-Planck equation derived from quasilinear theory, including a model lower hybrid diffusion term, an electron cyclotron term, a collision term, and a model transport term which describes the extraction of particles from the tail of the electron distribution function. Although it is easily demonstrated that the quasilinear equation with a Fokker-Planck collision term preserves the number of particles, the propagation of numerical errors may gradually modify this quantity. Therefore, we renormalize the distribution function at each time step of the numerical solution, in order to guarantee that the number of particles is locally preserved as required. The theory is applied to a slab of plasma, with parameters described by profiles typical of tokamaks. The objective of this simplified scheme is to emphasize the

dynamics in momentum space during the current drive with self consistent description of the electron cyclotron wave-particle interaction, in the presence of fast particle losses, and the resulting effect on the electron cyclotron absorption coefficient.

The plan of the paper is the following. In section 2 we present the quasilinear diffusion equation for the electron distribution function, with a short explanation on the lower hybrid and electron cyclotron diffusion terms, the collision term, and the term describing fast particle losses. In section 3 the results of a numerical analysis are presented and discussed. Section 4 summarizes the results and conclusions.

II. Quasilinear Theory for Time Evolution of the Electron Distribution Function

We will consider a simplified tokamak model, described by a slab of plasma, with the following profiles [17]

$$n_e(x) = n_e(0)\left(1-\frac{x^2}{a^2}\right)$$

$$T_e(x) = T_e(0)\left(1-\frac{x^2}{a^2}\right)^2 \qquad (1)$$

$$B_0(x) = B_0(0)\left(1+\frac{x}{R}\right)^{-1},$$

where a is the minor radius, R is the major radius, and x is the radial coordinate in the equatorial plane, with the origin in the center of the plasma column. $n_e(0)$, $T_e(0)$, and $B_0(0)$ are respectively the electron density, the electron temperature, and the ambient toroidal magnetic field, at the center of the plasma.

The time evolution of the electron distribution function, in a given point of the proposed slab geometry, under the action of lower hybrid and electron cyclotron waves, collisions and the loss term, may be described by the following equation

$$\partial_\tau f = (\partial_\tau f)_{lh} + (\partial_\tau f)_{cy} + (\partial_\tau f)_{col} + (\partial_\tau f)_{l} \qquad (2)$$

where $f = f(u_{||}, u_\perp, \tau, x)$. τ is the time normalized to the collision time, defined as the inverse of the collision frequency at the plasma center, $\nu_e(0) = 2\pi e^4 n_e(0)\Lambda(0)/m_e^{1/2}T_e^{3/2}(0)$. m_e is the electron mass, -e the electron charge, and $\Lambda(0)$ is the Coulomb logarithm at position x = 0. The $u_\perp$ and $u_{||}$ quantities that appear as arguments of f are the components of the momentum, normalized to $(m_e T_e(0))^{1/2}$, in the directions parallel and perpendicular to the ambient magnetic field.

The first term in the right hand side of equation (2) describes the action of lower hybrid waves and can be written as

$$(\partial_\tau f)_{lh} = \partial_{u||}(D_{lh}\partial_{u||}f) \quad (3)$$

where the term D_{lh} is the lower hybrid diffusion coefficient and takes the form [18]

$$D_{lh}(u_{||}) = \frac{4\pi}{e^2 n_0 \Omega \Lambda |u_{||}|}\left(\left|\frac{B}{A}\right|\frac{|D_{11}D_{22}-|D_{12}|^2|^2}{|\partial D/\partial N|}S(N_{||})\right)_{N_{||}=\mu_e^{1/2}/u_{||}} \quad (4)$$

In the above expression Ω is the frequency of lower hybrid waves, and $\mu_e \equiv m_e c^2/T_e(0)$. The D_{ij} are defined by $D_{ij} = N_i N_j - N^2 \delta_{ij} + \varepsilon_{ij}$, where the ε_{ij} are the components of the cold plasma dielectric tensor. The terms A, B and D are defined by

$$A = |D_{13}D_{22} - D_{12}D_{23}|^2 + |D_{23}D_{11} - D_{12}^* D_{13}|^2 + |D_{11}D_{22} - |D_{12}|^2|^2$$

$$B = D_{11}D_{22} - |D_{12}|^2 + D_{11}D_{33} - |D_{13}|^2 + D_{22}D_{33} - |D_{23}|^2$$

$$D = \varepsilon_{11}N_\perp^4 + N_\perp^2[(\varepsilon_{11}+\varepsilon_{33})(N_{||}^2 - \varepsilon_{11}) - \varepsilon_{12}^2] + \varepsilon_{33}[(\varepsilon_{11} - N_{||}^2)^2 + \varepsilon_{12}^2] = 0.$$

In these expressions $\mathbf{N} = c\,\mathbf{K}/\Omega$ is the vectorial refraction index for lower hybrid waves, where c is the speed of light, and $\mathbf{K}$ is the wave vector. The quantity $S(N_{||})$ is the spectrum of energy flux for the lower hybrid waves, written as a function of the wave electric field amplitude as follows

$$S(N_{||}) = \frac{c}{16\pi}\frac{|E|^2|\partial D/\partial N|}{|B|}. \quad (5)$$

Following what has been done in previous studies on quasilinear evolution due to lower hybrid waves [19], the spectrum of energy flux is modeled by the following expression where $S_0 = \int dN_{||} S(N_{||})$. When this model spectrum is utilized in the quasilinear equation the diffusion coefficient becomes nearly constant between $u_1 = \sqrt{\mu_e}/N_2$ and $u_2 = \sqrt{\mu_e}/N_1$, similarly to the flat plateau frequently employed as a cruder approximation. The shape of the lower hybrid diffusion coefficient as a function of parallel velocity and its dependence on plasma parameters can be appreciated in a previous publication dealing with the subject [19].

The term due to electron cyclotron waves appearing in equation (2) is given by [20, 11, 12]

$$(\partial_\tau f)_{cy} = \frac{1}{u_\perp}\left(Y\frac{\partial}{\partial u_\perp} + \frac{u_\perp}{\sqrt{\mu_e}}\frac{\partial}{\partial u_{||}}n_{||}\right)\left[u_\perp D_{cy}\left(Y\frac{\partial}{\partial u_\perp} + n_{||}\frac{u_\perp}{\sqrt{\mu_e}}\frac{\partial}{\partial u_{||}}\right)f\right], \quad (7)$$

where $Y = |\Omega_e|/\omega$, $\Omega_e = -eB_0/(m_e c)$ is the cyclotron angular frequency for electrons, and $\omega = 2\pi f_\omega$, f_ω being the wave frequency. B_0 is the local magnitude of the ambient magnetic field, and $n_{||}$ is the parallel component of the vectorial refraction index for electron cyclotron waves, $\mathbf{n} = c\mathbf{k}/\omega$.

The diffusion coefficient for electron cyclotron waves at the position x in a tokamak described approximately by a plasma slab can be written as follows, assuming a Gaussian distribution of parallel wave numbers [20]

$$D_{cy} = \frac{\alpha h \Gamma(n_{||})}{\gamma |u_{||}|}, \quad (8)$$

where

$$\alpha = \frac{4\pi}{e^2}\frac{P_0}{Sn_e \Lambda \omega},$$

$$h = \frac{c}{\omega}|b||\pi\cdot\sigma|^2 e^{-2\int_{x0}^{xk_\perp} "dx'},$$

and

$$\Gamma(n_{||}) = \frac{e^{-(n_{||} - \bar{n}_{||})2/(\Delta n_{||})2}}{\sqrt{\pi}\,\Delta n_{||}}$$

P_0 is the wave power at the initial position of the slab, $\gamma = \sqrt{1+u^2/\mu_e}$, $\bar{n}_{||} = \sin\bar{\Psi}$, and $\Delta n_{||} = \sin\Delta\psi$. $\bar{\Psi}$ is the injection angle of the central ray of the spectrum, relative to the normal to the ambient magnetic field. Explicit expressions for the quantities |b| and $\pi\cdot\sigma$ can be found in the literature [20, 12]. Moreover, the quantity $S = 4\pi^2 Rr$ is the magnetic surface of radius r. This quantity is introduced here because, even using the slab approximation, the formulation used for the diffusion coefficient takes into account the intersection between the radiation wavefront and the magnetic surface, which provides information about the fraction of time along which an electron moving on the magnetic surface remains under the influence of the waves [20].

The quantity $n_{\|}$ appearing in Eqs. (7) and (8) is the resonant value of the parallel wave number, $n_{\|} = (\gamma\text{-}Y)\sqrt{\mu_e}/u_{\|}$. $n_{\perp}$ is the perpendicular component of the vectorial refraction index. x_0 is the starting position of the cyclotron waves entering the plasma slab. The quantity h therefore is dependent upon the wave power in the position x, which depends on the absorption coefficient evaluated self-consistently along the time evolution of the distribution function.

For the collision term we use a simplified form that describes the interaction of electrons belonging to the tail with electrons from the body of the distribution function [11]. This term is given by

$$(\partial_\tau f)_{col} = \frac{Z+1}{u^3 \sin\theta}\,\partial_\theta [\,\sin\theta \partial_\theta f\,] + \frac{2}{u^2}\,\partial_u \left[\frac{1}{u}\,\partial_u f + f \right], \quad (9)$$

where θ is the angle between the particle momentum and the ambient magnetic field.

The last term in the quasilinear equation must describe the losses of particles from the system, intending to simulate locally the effect due to transport processes. These processes can be very complex, and for the present investigation we will satisfy ourselves with the study of the effect of finite confinement time on the evolution of the electron distribution function in momentum space. It is therefore sufficient to assume a simplified term for energetic particle losses, given by the following expression [2]

$$(\partial_\tau f)_l = \frac{1}{u^2}\,\partial_u \left[\frac{u^3}{2\,\nu_e(0)\,t_c} f \right] \quad (10)$$

where t_c is the confinement time of energy. It can be shown that this term describes an exponential decay of the kinetic energy of tail electrons.

The solution of the quasilinear equation (2) is possible only numerically. The absorption coefficient for electron cyclotron waves is evaluated by solving the dispersion relation for high frequency electromagnetic waves in a locally homogeneous magnetized plasma,

$$\det \left[k_i k_j - k^2 \delta_{ij} + \frac{\omega^2}{c^2}\,\varepsilon_{ij} \right] = 0, \quad (11)$$

where the k_i are the wave vector components, and the ε_{ij} are components of the warm plasma dielectric tensor. These are written in the small Larmor radius approximation, for waves with frequencies near the electron cyclotron frequency, keeping thermal and relativistic effects. A Maxwellian distribution is assumed for the evaluation of the Hermitian parts of ε_{ij}, while the anti-Hermitian parts, more sensitive to details in the distribution function, along the resonance curves, are numerically evaluated for the actual time-dependent distribution function obtained from the quasilinear diffusion

equation. As a consequence of the slab model utilized, the parallel component of the wave vector is constant along propagation of the wave. For a real wave frequency, the solution of the dispersion relation (11) is the complex quantity $k_\perp$.

III. Numerical Results

In order to solve numerically equation (2), we have written it as function of the variables u and $\mu = \cos\theta$, with the (u,μ) space described by a discrete grid of 201 × 101 points. The u limits of the grid are $u = 0$ and $u = u_{lim} = 15$ (u_{lim} is considerably greater than the upper limit of the lower-hybrid spectrum), and the limits in μ are $\mu = \pm 1$. It is assumed that the distribution remains Maxwellian at $u = u_{lim}$ and beyond, and satisfy the condition $\partial f/\partial\theta = 0$ at $\mu = -1$ and $\mu = 1$. The set of finite difference equations obtained from the quasilinear equation has been solved numerically, by using the alternating directions implicit method (ADI) [21]. In order to assure the required conservation of number of particles we introduce a renormalization procedure at each time step. We assumed the lower hybrid frequency to be $\Omega = 1$ GHz, with the spectrum such that $u_1 = 2.5$ and $u_2 = 7.5$. For the description of the plasma, we use parameters typical of small tokamaks, central electron density $n_e(0) = 1\times10^{13}$ cm^{-3}, central electron temperature $T_e(0) = 0.5$ kev, magnetic field at the center $B_0(0) = 1.5$ T, with a = 20 cm as the radius of the plasma column, and R = 100 cm as the torus radius.

For electron cyclotron waves we consider low-field side launching with f = 33.5 Ghz, with a Gaussian dispersion in parallel wave number. With this value of frequency we have $f \simeq 0.957 f_c$ at x = a, where f_c is the electron cyclotron frequency, and therefore we avoid the extraordinary mode cut-off inside the plasma. The central ray propagates at an angle $\bar{\Psi}$ relative to the normal to the magnetic field direction. In what follows we consider $\bar{\Psi} = -30^0$, and in all cases we take the same spread of the wave packet, $\Delta\bar{\Psi} = 3^\circ$, because it has been verified that, while the electron cyclotron absorption by an extended tail increases slightly with the width of the spectrum, the increase is not significant and is not enough to increase the asymptotic absorption coefficient beyond the value at the onset of the cyclotron irradiation, even in the absence of the loss term [12]. We consider also in what follows the effective ionic charge Z = 1, and the incident power of EC waves is taken as $P_0 = 0.05$ Mwatts.

The numerical analysis proceeds as follow: the electron distribution function evolves with lower hybrid waves, collisions and the energy loss term generating an extended tail. After a stationary state has been obtained the electron cyclotron waves are introduced in the system, assuming a constant value of P_0, while the other terms remain constant. A new stationary state is obtained after several collision times (around 200 collision times). The following figures refer to this asymptotic stationary state.

Initially, we study the parallel distribution function and the perpendicular temperature, defined respectively, as

$$f_{\|}(u_{\|}, \tau, x) = 2\pi \int_0^{\infty} du_{\perp}\, u_{\perp}\, f(u_{\|}, u_{\perp}, \tau, x) \qquad (12)$$

$$T_{\perp}(u_{\|}, \tau, x) = \frac{2\pi T_e}{f_{\|}} \int_0^{\infty} du_{\perp}\, u_{\perp} \frac{u_{\perp}}{2} f(u_{\|}, u_{\perp}, \tau, x),$$

considering that the lower hybrid waves energy density is $S_0 = 5$ W cm^{-2}, for $|x| < r_{lh} = 10$ cm (the central region of the plasma column), and $S_0 = 0$ for $|x| > r_{lh} = 10$ cm. Fig. 1a shows the parallel distribution function for position x = 10 cm, for the asymptotic stationary state (attained around $\tau = 400$ collision times) and several values of energy confinement time, $t_c = 1\times10^{-3}$ s, $t_c = 5\times10^{-3}$ s, $t_c = 1\times10^{-2}$ s, and $t_c = \infty$, which in terms of the normalized time are given respectively by $\tau \simeq 75$, $\tau \simeq 373$, $\tau \simeq 745$, and $\tau = \infty$. These values correspond for our parameters to a range varying nearly from Bohm diffusion time ($\simeq 1\times10^{-3}$ s) to the perfect confinement case, including the neo-Alcator scaling ($\simeq 5.6\times10^{-3}$ s) and the Goldston's scaling for ohmic discharges ($\simeq 3.8\times10^{-3}$ s). These values can be easily obtained using the following expressions obtained in the literature

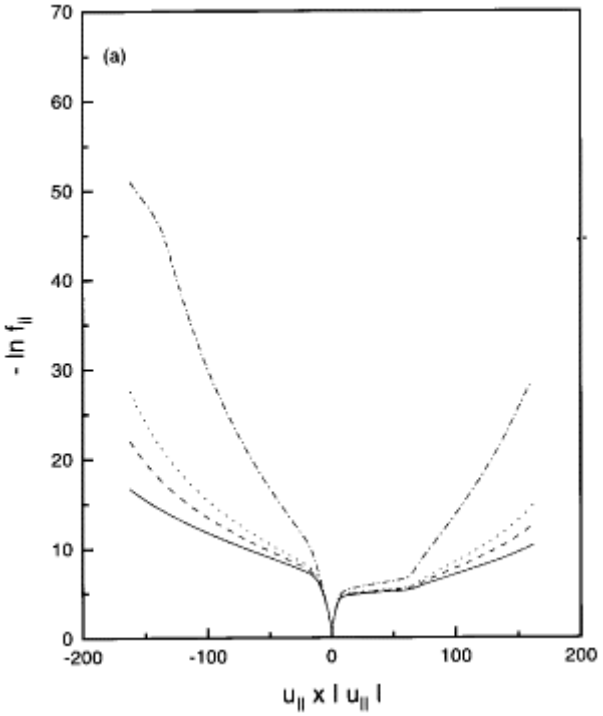

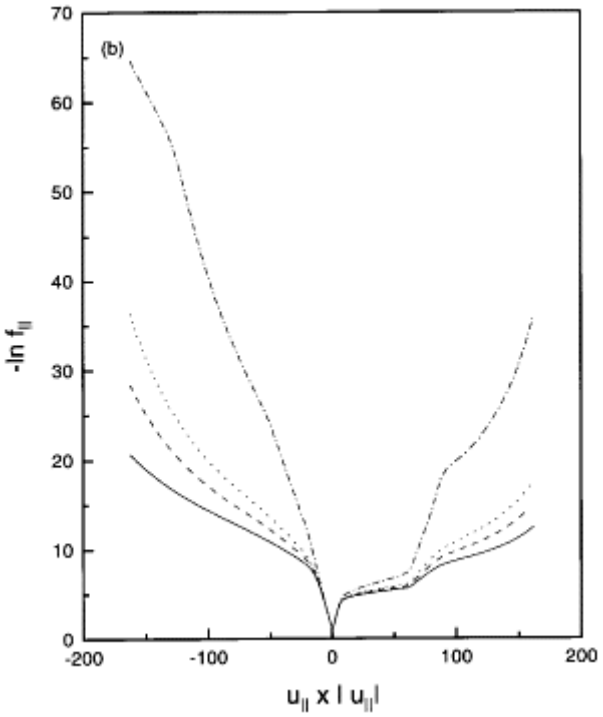

Figure 1. -ln $f_{||}$ vs $u_{||}\times|u_{||}|$, for $u_1 = 2.5, u_2 = 7.5$, $n_e = 1.\times10^{13}$ cm^{-3}, $T_e = 0.5$ kev, $B_0 = 1.5$ T, $\tau = 400$, and several values of the energy confinement time: $t_c = \infty$ (solid line), $t_c = 1\times10^{-2}$ s (dashed line), $t_c = 5\times10^{-3}$ s (dotted line) and $t_c = 1\times10^{-3}$ s (dot-dashed line). (a) x = 10 cm, (b) x = 4.23 cm.

Bohm diffusion time [22]:

$$\tau_E = 8\ a^2\ B/T_e \qquad (T_e\text{: eV, B: T; a: m})$$

Neo-Alcator diffusion time [23]:

$$\tau_E = 7\times10^{-22}\ n\ a\ R^2\ q \qquad \text{(SI units)}$$

Goldston diffusion time [24]:

$$\tau_E = 7.1\times10^{-22}\ n\ a^{1.04}\ R^{2.04}\ q^{0.5} \qquad \text{(cgs units)}$$

For Goldston and Neo-Alcator scalings we have assumed q = 4 as the safety factor.

It is seen in Fig. 1a that an extended tail has been formed in the side of positive values of $u_{||}$, and that particles from this extended tail have been collisionally scattered toward the backward propagating region of the momentum space. The population in the far tail, above the limit of direct influence of the lower hybrid waves, is also significantly enhanced by collisional processes. The time evolution (which we did not show for the sake of saving space) shows that an extended tail is quickly formed in the side of positive values of $u_{||}$, and that particles from this extended tail are later on collisionally diffused toward the backward propagating region of the momentum space. The loss

term competes effectively with the collisions in the high momentum region, and Fig. 1a shows the large effect of depletion of the population in the far tail and in the backward propagating tail, for the smaller values of t_c.

Fig. 2a depicts the corresponding stationary profile of the perpendicular temperature vs. $u_{||}$, for x = 10 cm. A large temperature peak has been formed in the side of positive values of $u_{||}$, centered around the extremity of the lower hybrid tail. At position x = 10 cm, the extremity of the lower hybrid tail is where is more significant the cyclotron absorption. Another temperature peak is formed in the backward tail, by collisional diffusion. The magnitude of the backward peak is comparatively smaller, for smaller confinement time, due to the competition between the loss term and the collision term. These temperature peaks are well known features from quasilinear diffusion due to lower hybrid waves interacting with electron cyclotron waves.

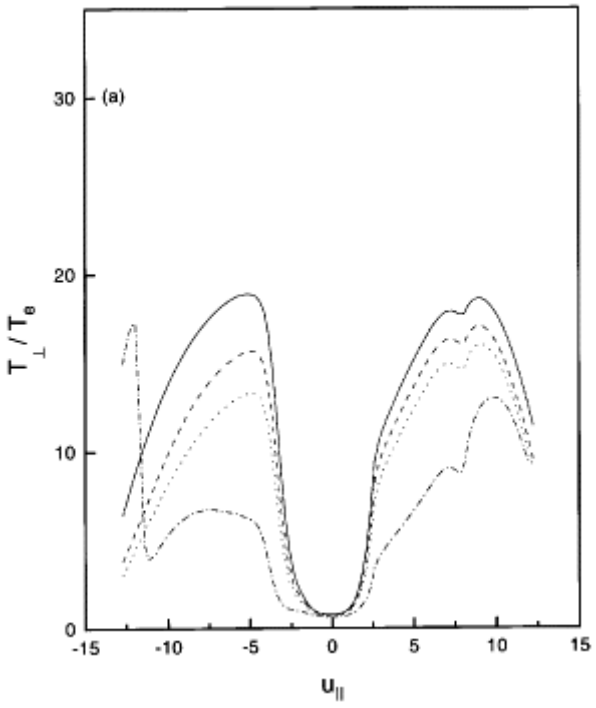

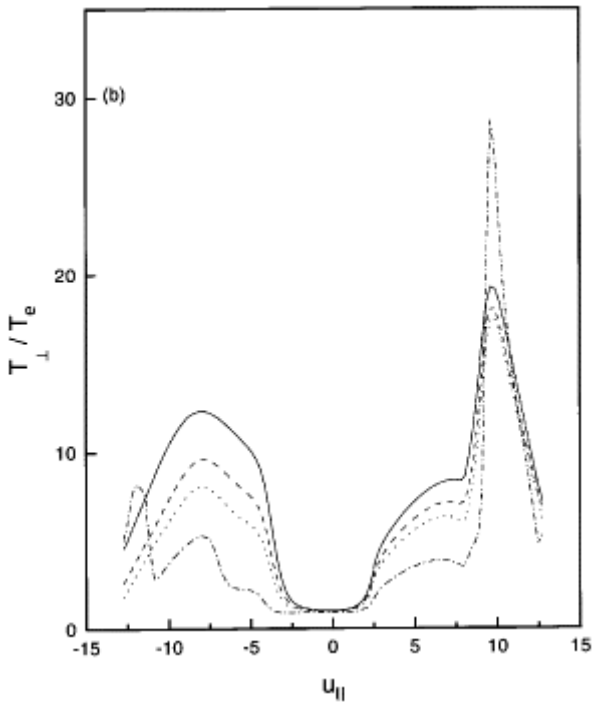

Figure 2. $T_\perp/T_e$ vs $u_\parallel$ for the same parameters and conditions of Fig. 1 ((a) x = 10 cm, (b) x = 4.23 cm).

Figs. 1b and 2b show respectively the parallel distribution function and perpendicular temperature at position x = 4.3 cm. At this position, the cyclotron resonance for the central ray of the wave packet is located at $u_\parallel \simeq 10$. The cyclotron absorption is above the LH tail, causing a modification in the parallel distribution which can be observed by comparing Fig. 1a and Fig 1b. Since the cyclotron energy is mainly given in the perpendicular direction in momentum space, and since the efficiency of collisions is smaller for higher momentum, the temperature peak shown in Fig. 2b for x = 4.3 cm is considerably larger than that shown in Fig. 2a, for x = 10 cm.

These results show that the asymptotic stationary state is qualitatively similar for the whole range of t_c values considered, but the tail population is considerably reduced by the decrease in the confinement time, as well as the anisotropy between parallel and perpendicular temperatures. These features can be very significant for the efficiency of cyclotron absorption, which is very sensitive to the population along the resonance curves.

In order to study the absorption coefficient for electron cyclotron waves (which is given by $\alpha = 2k_\perp''$, where $k_\perp''$ is the imaginary part of the electron cyclotron wave vector) we have restricted our interest to the case of extraordinary mode waves interacting with electrons in the tail of the distribution function, where the effect of the fast particle losses is more pronounced. The extraordinary mode at down shifted frequencies and oblique propagation is well absorbed by current carrying distributions [25]. As we have already mentioned, for the parameters chosen, the absorption around position x = 10 cm occurs mostly by electrons with velocities near 7.5 thermal velocities in the parallel direction. As the wave propagates inside the plasma the region of interaction shifts toward regions of higher parallel velocity.

As it is known, the asymptotic value of the absorption coefficient due to tail electrons is the outcome of a delicate balance, which in the present case occurs between diffusion due to lower hybrid and electron cyclotron waves, collisions, and the confinement properties, which affect the tail population. While lower hybrid waves populate the tail by dragging particles from the body of the distribution to the extremity of the tail and electron cyclotron waves push particles in the direction perpendicular to the ambient magnetic field, collisions tend both to diffuse particles along the pitch angle and bring the particles back to the body of the distribution by the effect of the so called collision drag, and ultimately tend to bring the distribution function back to a Maxwellian state. When a transport term is present, there is another mechanism for extraction of particles from the tail region. As a consequence, the decrease of the cyclotron absorption coefficient is expected, due to the decrease in the resonating population. The magnitude of this effect is shown in Fig. 3, where it is represented the asymptotic value of $k_{\perp}^{''}$ as a function of position in the plasma slab, for several values of t_c. Fig. 3a shows the case of a ray at the center of the cyclotron spectra ($n_{\parallel} = -0.5$), and Fig. 3b the case of another ray, located at the wing of the spectrum ($n_{\parallel} = -0.29$). The absorption for this value of $n_{\parallel}$ is mainly due to electrons ahead of the extremity of the lower hybrid tail, at $x \simeq 10$ cm, while the central ray is absorbed by electrons at the tip of the tail ($u_{\parallel} \simeq 7.5$). The comparison between Figs. 3a and 3b shows that both rays have nearly the same absorption coefficient at x = 10 cm, for perfect confinement, while the absorption coefficient for the ray at the spectral wing is considerably smaller than that for the central ray, at same position, for $t_c = 1.0\times10^{-3}$ s. This is due to the deleterious effect over the resonant population at large momentum, illustrated in Figs. 1a and 2a. A general observation extracted from Figs 3a and 3b is that the maximum of the absorption coefficient is seen to increase with the confinement time, as expected, and that the extension of the region where the absorption is significant increases toward the high-field side, as t_c is increased.

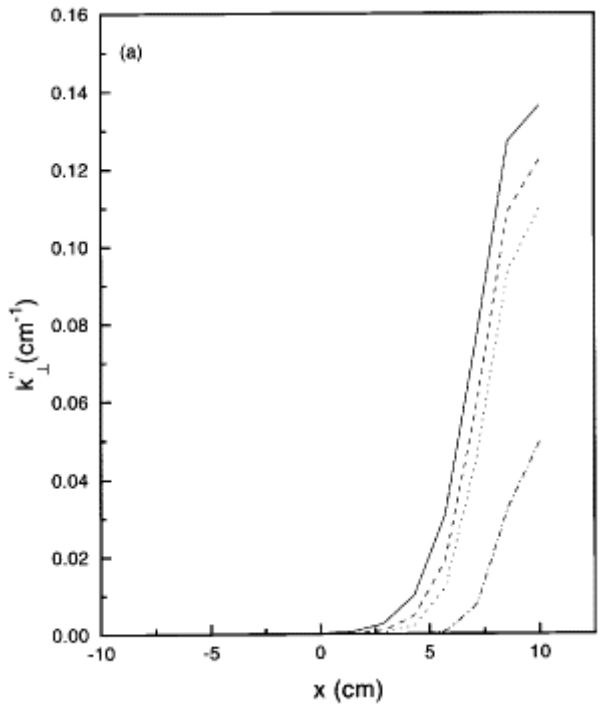

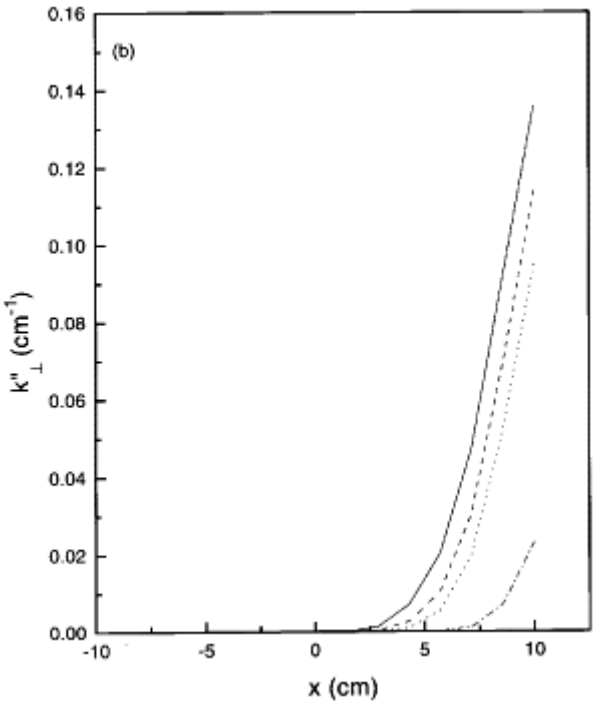

Figure 3. Imaginary part of the wave vector vs position, for the extraordinary mode with f = 33.5 Hz, for equatorial launching from the low-field side. (a) $n_{\|}$ = -0.5 (b) $n_{\|}$ = -0.29. Other parameters and conditions as in Fig. 1.

The effect of fast particle losses on the absorption coefficient can be appreciated from a different point of view in Fig. 4, where it is plotted the value of $R_{k\perp}$ against position in the plasma slab, for several values of t_c. $R_{k\perp}$ is defined as the ratio between $k_{\perp}''$ evaluated for a given confinement time t_c and $k_{\perp}''$ for the case $t_c = \infty$. It is seen from Fig. 4a, which refers to central ray of the spectrum, that for all points in the plasma slab the absorption coefficient for finite t_c is smaller than the value for $t_c = \infty$. For instance, Fig. 4a shows that, at position x = 10 cm, the absorption coefficient for the case of $t_c = 1\times10^{-2}$ is nearly 90 % of the value for infinite confinement time, while for the case of $t_c = 1\times10^{-3}$ s the ratio $R_{k\perp}$ is only nearly 35 %. The values of $R_{k\perp}$ are considerably reduced for positions closer to the plasma center. The meaning of this is made clear when we consider that at position x $\simeq$10 cm, one of the extremities of the resonant ellipse for the central ray of the cyclotron wave packet is located in momentum space near the extremity of the tail formed by lower hybrid waves ($u_{\|} \simeq 7.5$), while, for instance, at x $\simeq$ 4 cm it lies at $u_{\|} \simeq 13.4$. These values can be found in Fig. 5, where it is depicted the value of u_+, for the central ray ($n_{\|}$ = -0.50) and for rays at extremities of the Gaussian package ($n_{\|}$ = -0.71 and -0.37), against position in the plasma slab. u_+ indicates the extremity of the resonant semi-ellipse, which is the region in momentum space where the wave mostly interacts with the electrons, and is given by

$$\frac{u_{\pm}}{\sqrt{\mu_e}} = \frac{n_{\|}Y \pm \sqrt{n_{\|}^2 - 1 + Y^2}}{1 - n_{\|}^2},$$

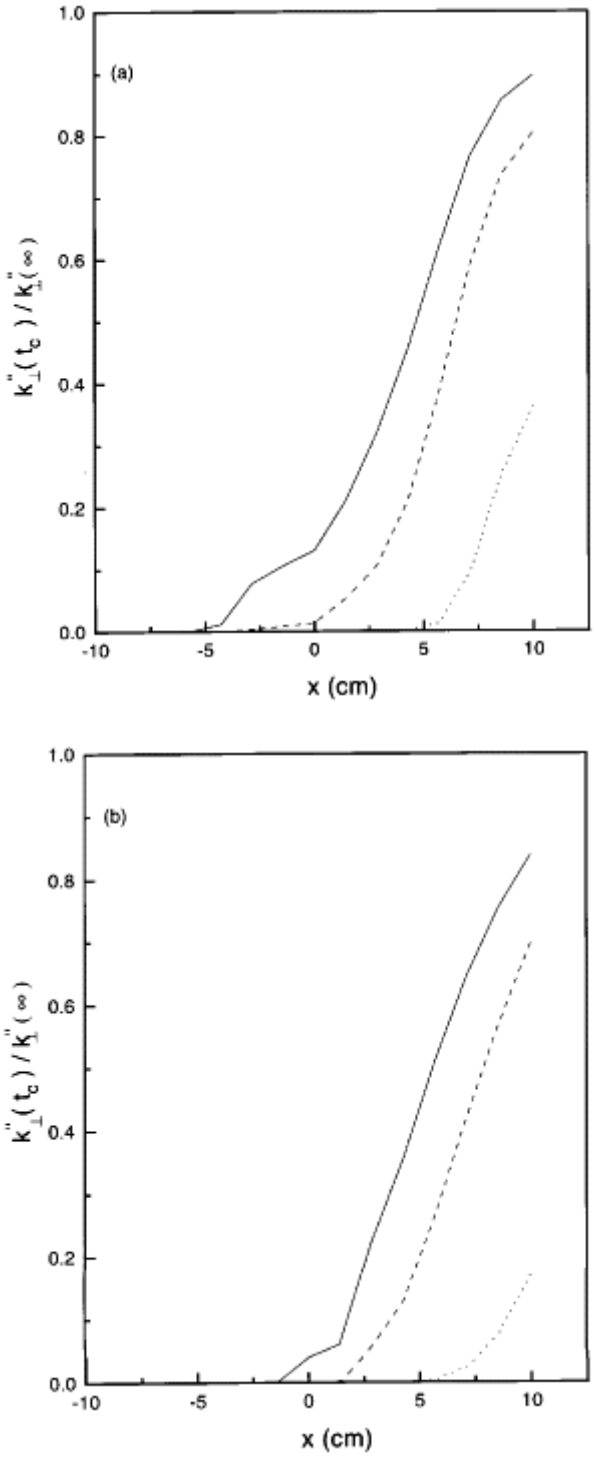

Figure 4. $R_{k\perp} = k_{\perp}''(t_c) / k_{\perp}''(t_c = \infty)$ vs position, for the extraordinary mode and stationary state, and several values of the energy confinement time: $t_c = 1\times10^{-2}$s (solid line), $t_c = 5\times10^{-3}$s (dashed line), $t_c = 1\times10^{-3}$s (dotted line). (a) $n_{\|} = -0.5$ (b) $n_{\|} = -0.29$. As in Fig. 3, the launching is equatorial from the low-field side, with f = 33.5 Hz. Other parameters and conditions as in Fig. 1.

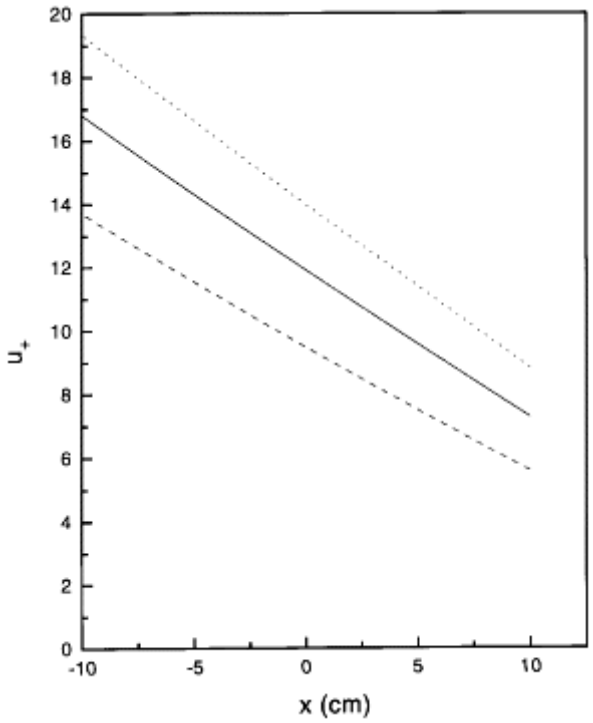

Figure 5. Position in momentum space where lies the extremity of the resonant ellipse, normalized to the thermal momentum at the center of the plasma slab (u_+), as a function of position in the plasma slab, for f = 33.5 GHz. $n_{||}$ = -0.5 (solid line), -0.71 (dashed line), and -0.37 (dotted line).

The other extremity of the ellipse is located at u_-, far away in the negative region of $u_{||}$, where practically there are no particles. Fig. 4b shows the ratio $R_{k\perp}$ for the ray with $n_{||}$ = -0.29, for which the interaction happens mainly for electrons beyond the extremity of the lower hybrid tail. As a consequence, the absorption coefficient is more strongly sensitive to the influence of the loss term. Fig. 4b shows that the reduction in the absorption coefficient for this ray in the wing of the Gaussian packet is more significant than for the central ray. While for position x = 10 cm the absorption coefficient for $t_c = 1\times10^{-2}$ is 85 % of the perfect confinement (close to the 90 % figure obtained for the central ray, as shown in Fig. 4a), for $t_c = 1\times10^{-3}$ the value of the ratio $R_{k\perp}$ is reduced to less than 20 %.

Fig. 4 therefore shows the relative magnitude of the effect of particle losses at the tail extremity over the cyclotron absorption coefficient, as compared to the effect of losses closer to the body of the distribution. For the case considered, in which we assumed confinement times ranging between Bohm diffusion time and perfect confinement (1 ms $\leq t_c \leq \infty$), the effect over the absorption by the extremity of the tail, shown in Fig. 4a near x = 10 cm, has been a modification by a factor of nearly three. For waves interacting with particles beyond the extremity of the tail, which is collisionally populated, the reduction of the absorption with the decrease of confinement time is much more impressive, as can be seen in Fig. 4a for decreasing values of x, and in fig. 4b for the whole range of x.

A different point of view for the same subject can be found in Fig. 6, where it is shown the dependence of the absorption coefficient with parallel wave number, for several

values of t_c, at position x = 10 cm. It is seen that for decreasing values of the confinement time there is a decrease of the values of the absorption coefficient, relative to the case $t_c = \infty$, for all values of $n_{||}$ in the range considered. Moreover, one notices for the case of perfect confinement that the quasilinear flattening of the distribution produced by EC waves causes a localized reduction of the absorption coefficient of the central ray ($n_{||} = -0.5$), which carries the maximum power. This effect of localized reduction of the absorption coefficient gradually becomes less noticeable with the decrease of t_c, because the loss term acquires more influence and contribute to obliterate the effect of the EC waves.

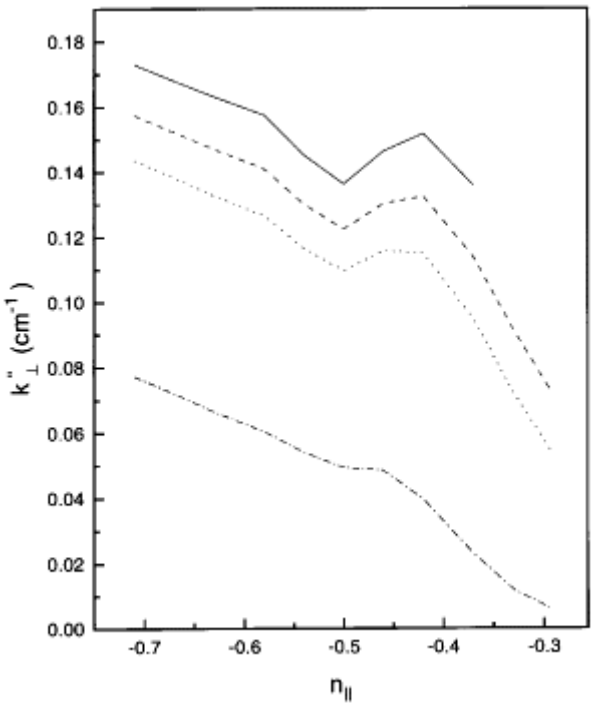

Figure 6. $k_{\perp}''$ versus $n_{||}$, at position x = 10 cm, for perfect confinement (solid line), $t_c = 1\times10^{-2}$ s (dashed line), $t_c = 5\times10^{-3}$ s (dotted line) and $t_c = 1\times10^{-3}$ s (dot dashed line). As in Fig. 3, the launching is equatorial from the low-field side, with f = 33.5 Hz. Other parameters and conditions as in Fig. 1.

It is interesting to observe also the dependence of the integrated absorption on the confinement time. The integrated absorption gives the fraction of incident energy which arrives at position x inside the slab, and is defined as

$$\eta(x) = 1\text{-}\exp\left(-2\int_{x_0}^{x} k_{\perp}''\,dx'\right).$$

The effects of finite energy confinement time over the integrated absorption are shown in Fig. 7, for the central ray of the spectrum. Fig. 7 shows that, for confinement time greater or equal 1×10^{-2} s, the integrated absorption is not significantly modified as

compared to the case of perfect confinement. For smaller confinement times, in the range of Goldston scaling or smaller (~ 1.9 $\times 10^{-3}$ s), the integrated absorption can be reduced to less than 50 % of the perfect confinement case. These results indicate the sensitivity of the integrated absorption to the confinement time, something which may be useful for the evaluation of the confinement regime by transmission measurements of cyclotron radiation.

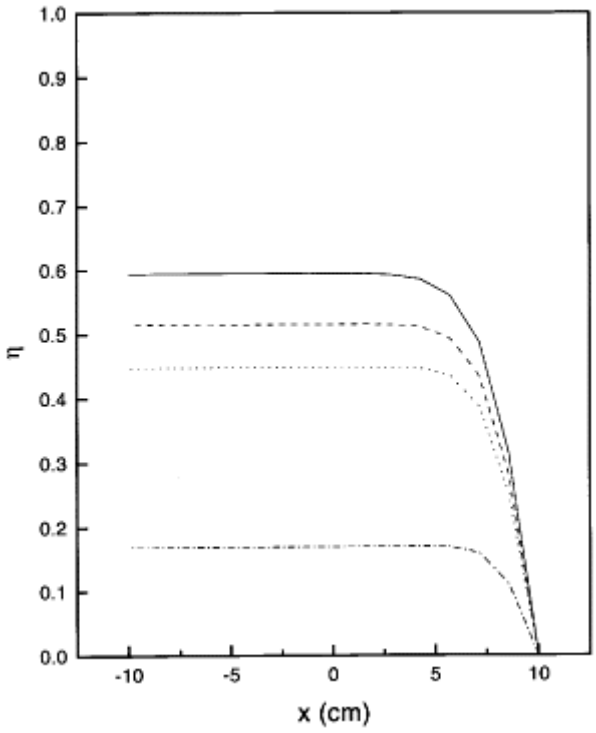

Figure 7. Integrated absorption (η) versus position in the plasma slab. Other conditions and conventions as in Fig. 6.

IV. Conclusions

In the present work we have investigated the behaviour of electron cyclotron absorption by a current carrying distribution produced by lower hybrid and electron cyclotron current drive, in the presence of fast particle losses which intend to simulate the effect of losses due to spatial transport. The study was conducted by numerically solving the quasilinear equation for the time evolution of the electron distribution function, under the effect of lower hybrid and cyclotron waves, collisions, and fast particles losses, assuming parameters typical of small tokamaks, described by a slab model. The absorption coefficient for electron cyclotron waves was self-consistently obtained with the use of the actual time-evolving distribution function in the evaluation of the anti-hermitian parts of the dielectric tensor.

The objective of these studies has been to improve the understanding of the effects of fast particle losses on the evolution of the electron distribution function and on the

cyclotron absorption coefficient by lower hybrid produced tails, in a situation where electron cyclotron waves are self-consistently affecting the dynamics of the system. The investigation shall continue by improving the description of the effect of transport processes, possibly incorporating in the quasilinear equation radial losses due to spatial diffusion [26].

The results obtained with the present investigation show important deleterious effects due to the particle losses, with reduction of the absorption coefficient for extraordinary mode waves propagating at large angles relative to the ambient magnetic field. The integrated absorption can suffer reduction of nearly 50 %, for absorption by electrons at the extremity of the lower hybrid produced tail, when the confinement time is changed from $t_c = \infty$ (perfect confinement) to a value of order of Bohm diffusion time. The results also show that the absorption of electron cyclotron waves by electrons beyond the extremity of the lower hybrid tail can be much more affected.

The behaviour of the absorption coefficient is related to the evolution of the electron distribution function. We have shown how the tail population is affected by the reduction in the confinement time, and how the collisionally populated counter streaming tail which evolves during lower hybrid current drive is substantially reduced. The perpendicular temperature profile typical of lower hybrid current drive is qualitatively similar to the case of perfect confinement, but the magnitude of the anisotropy among parallel and perpendicular temperatures is considerably reduced by effect of the finite confinement time, specially in the counter streaming region of momentum space.

The results obtained are appropriated for the case of large aspect ratio tokamaks, where the plasma slab approximation can be utilized, and for parameters typical of small tokamaks. For small aspect ratio tokamaks, toroidal effects must be added in order to find a more realistic description of the plasma. The qualitative conclusions should also apply to the case of large tokamaks, but a detailed numerical study should be conducted in order to arrive to quantitative conclusions about the effect of finite confinement time for a different range of parameters.

Acknowledgments

This work has been partially supported by the Brazilian agencies Conselho Nacional de Desenvolvimento Científico e Tecnológico (CNPq), Financiadora de Estudos e Projetos (FINEP). The numerical calculations were made in the Supercomputer Center installed at the Universidade Federal do Rio Grande do Sul (CESUP-UFRGS), and at the Laboratory of Special Projects at UFMS (LPE/UFMS). One of us (P.R.S.R) would like to acknowledge UFMS by financial support in all phases of this research.

References

[1] S. C. Luckhardt, Nuclear Fusion, **11**, 1914 (1987).

[2]
G. Giruzzi, V. Krivenski, I. Fidone and L. F. Ziebell, Plasma Phys. Contr. Fusion, **10**, 1151 (1985).
[3]
G. Giruzzi, I. Fidone, G. Granata and V. Krivenski, Nuclear Fusion, **10**, 662 (1986).
[4]
R. L. Meyer, I. Fidone, G. Giruzzi and G. Granata, Phys. Fluids, **28**, 127 (1985).
[5]
K. Ushigusa, T. Kondoh, O. Naito, Y. Ikeda, S. Ide, M. Seki, S. W. Wolfe, M. Sato, Y. Kamada, K. Itami and T. Imai, Nuclear Fusion, **32**, 1977 (1992).
[6]
G. Giruzzi, Plasma Phys. Contr. Fusion, **35**, 1541 (1993).
[7]
P. R. da S. Rosa and L. F. Ziebell, *Proceedings of the IAEA Technical Commitee Meeting, TCM/RUST, Serra Negra, Brazil*, 3-6 (1993).
[8]
J. L. Ségui and G. Giruzzi, Plasma Phys. Contr. Fusion, **36**, 897 (1994).
[9]
F. Skiff, D. A. Boyd and J. A. Colborn, Plasma Phys. Contr. Fusion, **36**, 1371 (1994).
[10]
N. J. Fisch and A. H. Boozer, Phys. Rev. Lett., **45**, 720 (1980).
[11]
V. Krivenski, and I. Fidone, G. Giruzzi, R. L. Meyer, and L. F. Ziebell, Phys. Fluids, **30**, 438 (1987).
[12]
P. R. da S. Rosa and L. F. Ziebell, Plasma Phys. Contr. Fusion, **35**, 511 (1993).
[13]
P. R. da S. Rosa and L. F. Ziebell, Plasma Phys. Contr. Fusion, **38**, 375 (1996).
[14]
G. Giruzzi, Plasma Phys. Contr. Fusion, **35**, A123-A139 (1993).
[15]
Y. Peysson, Plasma Phys. Contr. Fusion, **35**, B253-B262 (1993).
[16]
S. Texter, M. Porkolab, P. T. Bonoli, S. Knowlton and Y. Takase, Phys. Letters A, **175**, 428-432 (1993).
[17]
I. Fidone, R. L. Meyer and G. Granata, Phys. Fluids, **26**, 3292 (1983).
[18]
I. Fidone, G. Giruzzi, G. Granata and R. L. Meyer, Phys. Fluids, **27**, 2468 (1984).
[19]
P. R. da S. Rosa and L. F. Ziebell, Plasma Phys. Contr. Fusion, **34**, 533 (1992).
[20]
I. Fidone, G. Granata and R. L. Meyer, Phys. Fluids, **25**, 2249 (1982).
[21]
B. Carnahan, H. Luther, and J. Wilkes, *Applied Numerical Methods*, John Wiley, New York (1969).
[22]

F. F. Chen, *Introduction to Plasma Physics and Controlled Fusion*, Plenum, New York, 2nd. ed. (1984).

[23] B. B. Kadomtsev, F. S. Troyon and M. L. Watkins, Nucl. Fusion, **30**, 1675 (1990).

[24] R. B. White, *Theory of Tokamak Plasmas*, North Holland, Amsterdam (1989).

[25] I. Fidone, G. Giruzzi, V. Krivenski, E. Mazzucato and L. F. Ziebell, Nucl. Fusion, **27**, 579 (1987).

[26] A. G. Peeters and E. Westerhof, Phys. Plasmas, **3**, 1628 (1996).

Sociedade Brasileira de Física

Caixa Postal 66328
05315-970 São Paulo SP - Brazil
Tel.: +55 11 3091-6922
Fax: (55 11) 3816-2063
e-Mail
sbfisica@sbfisica.org.br